# Conodont stratigraphy and biodiversity of the Middle Devonian Kačàk Episode in the Pic de Bissous (Montagne Noire, S-France)

**Katarzyna Narkiewicz**

katarzyna.narkiewicz@pgi.gov.pl

Polish Geological Institute-National Research Institute: Panstwowy Instytut Geologiczny Panstwowy Instytut Badawczy https://orcid.org/0000-0003-1072-0987

**Marek Narkiewicz**

Polish Geological Institute-National Research Institute: Panstwowy Instytut Geologiczny Panstwowy Instytut Badawczy

**Research Article**

**Keywords:** Kačàk Episode, conodont zonation, biodiversity change, juvenile mortality, eustatic change

**Posted Date:** May 14th, 2024

**DOI:** https://doi.org/10.21203/rs.3.rs-4242174/v1



**Version of Record:** A version of this preprint was published at Palaeobiodiversity and Palaeoenvironments on December 12th, 2024. See the published version at https://doi.org/10.1007/s12549-024-00632-3.

# Abstract

Pic de Bissous belongs to classic sections of the latest Eifelian Kačàk Episode (KE) interval, uniquely developed in hemipelagic carbonate facies. The present conodont study is based on dense sampling of the section, yielding rich and diverse assemblages dominated by *Polygnathus*. The position of the lower and upper KE boundaries is here documented within the late Eifelian *kockelianus* Zone and at the base of the lowermost Givetian *hemiansatus* Zone, respectively. Both boundaries are marked by an increase of $P_1$ elements diversity, the phenomenon reported also from other palaeogeographic setting, and accompanied by an appearance of several new taxa. This suggests a global two-step conodont biodiversity rise around the KE interval, presumably caused by the eustatic If and earliest Givetian sealevel rise, respectively. These events were accompanied by increased juvenile conodont mortality probably due to some local/regional adverse conditions of either abiotic or biotic nature.


# Introduction

The latest Eifelian Kačák Episode (KE) is one of several Devonian turning points marked by black-shale levels, such as the Kellwasser or Hangenberg events (Walliser 1996; House 2002; Kabanov and Jiang 2020). Recently, Narkiewicz et al. (2021) stressed its significance for understanding climatic and biotic geosystem perturbations, including global warming, humidization, eustatic events and development of incipient forests. Also, the crucial role of conodonts in a global correlation of KE has been reviewed and discussed as well as their importance in studying environmental aspects of the episode (Narkiewicz et al. 2023).

One of the key localities of the Kačák Episode is the Pic de Bissous section (Marbrière Nord Quarry) in the Montagne Noire area of southern France (House 1996). This classic section is particularly interesting as it demonstrates unique KE development in hemipelagic calcareous facies lacking typical black-shaly development. In spite of its importance, the Eifelian to lower Givetian part of the section lacks adequate biostratigraphic documentation. Only a few brief contributions have been published, devoted to cephalopods (House and Chlupáč, 1987) and conodonts (Walliser 1990, see also Feist 2002). Moreover, the conodont biofacies development has been summarized recently by Narkiewicz et al. (2023).

In this paper we present the comprehensive documentation and biostratigraphic interpretation of conodont fauna of the Eifelian-Givetian boundary interval in the Pic de Bissous section. Succession of conodont assemblages, their diversity, biofacies and proportion of juvenile elements are interpreted in terms palaeoenvironmental changes related to the Kačák Episode.

# Geological setting

The Pic de Bissous (Marbrière Nord Quarry) is located ca. 40 km west of Montpellier in southern France (Languedoc Province, present region of Occitanie). The coordinates of the quarry are: 43.601468 N, 3.356479 E. The exposed strata belong to the carbonate Pic-de-Bissous Group > 20 m thick, comprising

upper Emsian to lower Givetian (Feist 1985, 2002). House (1995) subdivided the section into informal “beds” labelled with capital letters (A-S). The measured part of the section consists of reddish to grey, pure to slightly marly homogenous limestones passing upwards into nodular “griotte”-type varieties (Fig. 1). The regular bedding is highlighted by horizontal clay seams and stylolite sutures. Macroscopic skeletal remains include mainly echinoderms, cephalopods (House and Chlupač 1987; House 1996), and trilobites (Feist 2003), while microscopic constituents are dominated by styliolinids, nowakiids and benthic ostracods.

During the Middle Devonian, the area was located near the northern Gondwana margin, approximately at 30$^{O}$S palaeolatitude (Golonka and Gawęda 2012). The detailed palaeogeographic-facies setting is difficult to reconstruct due to the Variscan tectonic overprint, however. The quiet-water hemipelagic regime with water depth below normal wave-base and located far from terrigenous sediment sources is consistent with sedimentological and palaeontological evidence available (Tucker 1973; Feist and Klapper 1985; Casier and Préat 1996; unpublished authors’ observations).

## Materials and methods

Conodonts for the present study were obtained from 20 samples weighting ca. 1 kg each, collected in January 2020 and in March 2022. They were processed in the PGI-NRI Micropaleontological Laboratory (Warszawa, Poland) using 15% formic acid for dissolution, and sodium polytungstate solution for heavy fraction enrichment. The conodont material totals more than 2500 generally well-preserved specimens including 2179 $P_1$ elements. The conodont frequency in a sample varies between 14 and 503, with and average 109 and most of the samples containing from 70 to 180 specimens (Fig. 1). Large percentage of juvenile $P_1$ forms, and a relatively high proportion of ramiforms testify to an autochthonous character of the studied assemblages.

The identification of particular taxa, especially the stratigraphically important ones, is based on original diagnoses and illustrated holotypes, the approach stressed in the earlier paper (Narkiewicz et al., 2023). The studied taxa were documented by SEM photographs. The assemblages comprised eight genera: *Polygnathus*, *Icriodus, Tortodus*, *Ozarkodina*, *Coelocerodontus*, *Belodella*, *Neopanderodus* and *Dvorakia*, ascribed to 37 lower order taxa and morphotypes. Majority of specimens belongs to *Polygnathus*, including up to 20 species and subspecies and four taxa determined in an open nomenclature.

The conodont biofacies succession, summarized by Narkiewicz et al. (2023), was supplemented by samples 21–23 from the upper part of the section. The uppermost sample 24 with its merely 14 $P_1$ specimens was not considered (Fig. 1). The methodology of the biodiversity analysis is presented in the respective section below.

# Taxonomic remarks

All the identified taxa and their frequency in the samples are listed in SM 1 whereas majority of taxa are illustrated in Figs. 2–5. The specimens determined on a generic level (e.g., *Polygnathus* sp., *Icriodus* sp. etc.) could not have been ascribed to particular species mainly because of a serious damage or extremely juvenile ontogenetic stage. The specimens labelled as *conformis*, e.g. *Icriodus* cf *I. hollardi* have recognizable specific features but at the same time their important part or platform ornamentation were damaged or they represent juvenile forms. Thus, they have to be treated with caution when applied for biostratigraphic purpose or for biodiversity analysis. The forms described as *affinis* (*Polygnathus linguiformis* aff. *mucronatus* and *Polygnathus* aff. *P. hemiansatus*) are similar to the respective taxa but they differ in at least one feature.

The representatives of the genus *Polygnathus* attain 80% of the whole $P_1$ collection, the most abundant forms being *P. parawebbi*, *P. linguiformis linguiformis* 1a and *P. linguiformis saharicus*. These taxa are present in most of the samples throughout the entire section studied. Notably, in contrast to the data in Walliser (1990) neither *P. ensensis* nor *P. eiflius* has been found in the Eifelian part of the Pic de Bissou section.

The taxa described as *affinis* or transitional forms are represented by a few, usually 1–2 specimens with the exception of a form described below as a new morphotype.

*Polygnathus pseudofoliatus* Wittekindt 1966 γ morphotype

Figure 4m, r; Fig. 5s

Diagnosis (according to Klapper 1971, p. 63): Representative specimens of *Polygnathus pseudofoliatus* have transverse ridges or transversely aligned nodes separated from the carina by adcarinal grooves. Platform is generally constricted anteriorly. Free blade is generally more than one third (up to one half) the total length of the unit.

Remarks: Walliser and Bultynck (2011) described α and β morphotypes of *Polygnathus pseudofoliatus*. Morphotype α strictly corresponds to the holotype, whereas morphotype β differs from α in having a narrower platform, more distinct rostrum in the anterior part of the platform, well-developed adcarinal grooves and ornamentation composed mainly of ridges. Morphotype α first appears in the *kockelianus* Zone while morphotype β already at the base of the *australis* Zone.

The Pic de Bissou assemblages comprise morphotype α (Fig. 2g, i, n; Fig. 4g, k, n) as well as β (Fig. 1m, r; Fig. 5s). New *Polygnathus pseudofoliatus* γ morphotype can display a platform outline similar as in both morphotypes (α - Fig. 3m; β – Fig. 4s). It differs from these, however, in distinctly higher anterior inner platform margin. This feature appears in younger, Givetian polygnathids: *Polygnathus denisbriceae*, *P. alatus* and *P. webbi*. In the above named species the right margin is higher than the left one in both right- and left-curved specimens. Unfortunately, our collection of the new morphotype includes only left-curved forms and therefore it is not certain if the discussed feature occurs also in the right-curved counterparts. *Polygnathus pseudofoliatus* γ morphotype differs from *P. denisbriceae* in having a distinctly wider

platform, particularly in its posterior part which does not form a pointed tip, and in posessing a more distinct ornamentation (see Brice et al. 1979). In *P. alatus* and *P. webbi* "the anterior outer platform margin is distinctly higher on the right side than on the left in both left-curved and right-curved specimens" (see Klapper and Lane 1985, p. 932). In both species the adcarinal grooves are fairly deep and continue to the platform termination.

Material: 11 specimens (SI 1).

Occurence: Pic de Bissou section, samples 14, 16, 17 from the *hemiansatus* Zone of the lowermost Givetian.

# Biostratigraphy

Stratigraphic ranges of particular taxa are here referred to the conodont zonation discussed by Narkiewicz et al. (2023; Fig. 1). The "*ensensis*" Zone has been put in quotation marks as the authors questioned the concept of the formal uppermost Eifelian *ensensis* biozone. It has been argued that the key subspecies *Polygnathus xylus ensensis* Ziegler and Klapper, 1976 has been found only in the Givetian so far. Figure 6 shows the stratigraphic ranges of conodonts from the Pic de Bisous section, partly based on Narkiewicz et al. (2023, Fig. 3). Their first and last appearance datums (FADs and LADs) were established based on own observations as well as on a critical review of the literature data (cited by Narkiewicz et al. 2023 and supplemented here). First appearances of *Polygnathus eiflius* Bischoff and Ziegler, 1957, P. *ling. klapperi* Clausen, Leuteritz and Ziegler, 1979d *amphora* Walliser and Bultynck, 2011 were reconsidered in the recent literature and therefore are discussed below.

The earliest occurrence of *Polygnathus eiflius* has been reported by Vodrážkova and Suttner (2020) from the *australis* Zone in the Jirásek Quarry section in Czechia. The single specimen of *P. eiflius* from the *australis* Zone illustrated by Vodrážkova and Suttner (2020, Fig. 9D) raises reservations, however. The specimen has a wide, distinctly concave platform and strongly fortified, short anterior platform margins with sharp edges (rostrum). The margins are joined by short ridges which seem to compose part of a platform ornamentation rather than extended rostrum margins forming diagonal ridges. The short rostrum and platform outline do not resemble the holotype (Bischoff and Ziegler 1957, pl. 7a, b) being more similar to the specimens included to *P. eiflius* from the *kockelianus* Zone (Weddige 1977, cf. detailed description in p. 312) and to the Givetian specimen illustrated by Weddige (1977, pl. 4, Fig. 66). The presence of *P. eiflius* in the *australis* Zone in the eastern margin of the Rhenish Slate Mts. (Vodrážkova and Suttner 2020 p. 18) is also doubtful as in the Hörre and Lahn-Mulde areas *P. eiflius* co-occurs with *Tortodus kockelianus* and *T. australis* which suggests erroneous determination of the latter species (Weddige 1977, Table 16, p. 390; Table 18, p. 394, respectively). In our opinion, extending FAD of *P. eiflius* based on a single non-typical specimen seems questionable. Moreover, the remaining morphologically variable specimens of *P. eiflius* illustrated by Vodrážkova and Suttner (2020, Fig. 9) cannot be considered as typical representatives of the species as well. The specimens with a broken anterior part (Fig. 9A, B) may not represent *P. eiflius* but some other species, e.g. *P. amphora* (compare

with Fig. 6H). The observations of the first author do not confirm the presence of *P. eiflius* neither in the collection of Jiří Kalvoda (Kalvoda 1992) nor in the own material from the Jirásek Quarry.

The literature data indicates that *P. eiflius* first appears in the upper part of the *kockelianus* Zone in Morocco. Typical specimens were found in the Jebel Mech Irdane section in sample 115 (Walliser and Bultynck 2011, Fig. 2; pl. 1, Fig. 6) just before the disappearance of the last representatives of *Tortodus kockelianus kockelianus*, and in the Bou Tchrafine section in sample 15a (Narkiewicz et al. 2023, Fig. 2E). In Germany *P. eiflius* is known from the upper Eifelian Odershausen Formation in the Blauer Bruch section (Schöne 1997), where it co-occurs with *T. kockelianus kockelianus* (Bischoff and Ziegler 1957, p. 24; Table 4, p. 132; sample 9, observations of the cited authors' collection by the first author).

The first appearance of *Polygnathus ling. klapperi* Clausen in the *kockelianus* Zone below the uppermost Eifelian, understood as the "*ensensis*" Zone here, was noted only by Vodrážkova and Suttner (2020). The concept of Vodrážkova and Suttner (2020) questioning the holotype of *Polygnathus ling. klapperi* Clausen et al. (1979, pl. 1, Fig. 7) is not accepted here, however. According to Vodrážkova and Suttner (2020) the holotype is not adequate to the diagnosis in having an elevated outer platform margin and too deep adcarinal grooves. Nevertheless, it may be noted that the outer margin is not higher than the inner one, and, importantly, it does not form a high flange-like margin. According to the original diagnosis, the adcarinal grooves may be deeper or shallower which is implied by the statement that "The outer anterior platform bears strong transverse ridges separated from the carina *by an adcarinal trough or groove…*" (Klapper 1977, p. 465; Clausen et al. 1979). We do not accept as the representatives of *P. ling. klapperi* the specimens with regularly curved outer margin of a platform, being widest in its middle part, and with a tongue which gently turns inward or is sharply bent downwards (Vodrážkova and Suttner 2020, Fig. 15). The platform of the holotype is widest just in front of the anterior part of the tongue that "turns inward in a sharply rounded curve" (Klapper 1977, p. 465; Clausen et al. 1979).

According to our observations the correctly identified representatives of *P. ling. klapperi* from the uppermost Eifelian are reported from Jebel Mech Irdane, sample 115 (Walliser and Bultynck 2011, Fig. 2 – specimen not illustrated), Jirásek Ouarry Bed 45 (Kalvoda 1992; collection of J. Kalvoda, confirmed by the first authors' inspection) and in the Pińsk 54 section, sample 95b (Narkiewicz et al. 2023, Fig. 2H). Contrary to the suggestion of Vodrážkova and Suttner (2020, p. 34) the taxon has not been reported from the *kockelianus* Zone in Morocco. In the Bou Tchrafine section its first appearance (not illustrated) has been noted from the "*ensensis"* Zone of the uppermost Eifelian (Walliser and Bultynck 2011, Fig. 3) while the illustrated, correctly identified specimen is from sample 19 attributed to the *hemiansatus* Zone (Bultynck and Hollard 1980, Fig. 3, pl. VII, Fig. 2). The inspection of the Pierre Bultynck collection from Jebel Ou Driss Eastern by the first author did not reveal any single representative of the discussed taxon.

Vodrážkova and Suttner (2020, Fig. 6B) reported the earliest occurrence of *Polygnathus amphora* from the *australis* Zone. Nevertheless, the illustrated specimen is not a typical representative of the species as it has a very high outer interior platform margin, significantly higher than the inner one, and thus it can be determined merely as "affinis". Typical forms have both anterior margins at the same level (compare the

holotype, Walliser and Bultynck 2011, pl. 1, Fig. 19). The species first appears in the upper *kockelianus* Zone, in sample 15 from the Bou Tchrafine section (Bultynck 1987, pl. 8, Fig. 8), as well as in samples 285 and Ji8 of the Jirásek Quarry (Vodrážkova and Suttner 2020, Fig. 6D and E, respectively).

The *kockelianus*, *hemiansatus* and *timorensis* zones have been defined in the studied section based on FADs of the zonal taxa and verified taxonomy and stratigraphic range of *Polygnathus ling*. *klapperi*. The *kockelianus* Zone is determined in the interval spanning samples 3 to 10 based on the occurrence of the key taxon *Tortodus kockelianus kockelianus* (Sl 1). In samples 3 and 4 the taxon is represented by early ontogenetic forms (Fig. 2r-t). In the upper samples also mature specimens were found (compare Fig. 3y, sample 8). The uppermost occurrence in sample 11, ascribed to the "*ensensis*" Zone, includes juvenile forms again (Fig. 3s). Notably, *Tortodus intermedius* is relatively frequent, representing initially juvenile forms (Fig. 2o-q, sample 4) replaced upwards by mature ones (Pl. 1, Fig. S, sample 7). According to Walliser and Bultynck (2011) *Polygnathus ling. saharicus* (Fig. 2a, sample 3), *P*. *pseudofoliatus* α morphotype (Fig. 2i, sample 4), *P*. *amphora* (Fig. 3w, sample 7A) and *P*. *ling. linguiformis* 3 (Fig. 2dd, sample 6) also have their FADs in the *kockelianus* Zone.

The assemblages from samples 11–12 may correspond to the "*ensensis*" Zone of the uppermost Eifelian, based on the presence of such characteristic taxa as *Polygnathus ling*. *klapperi* (Fig. 3t, sample 11) and *P. linguiformis* n. ssp. A (Fig. 3z, sample 12). The occurrence of the first taxon in the uppermost Eifelian was documented in the Belarusian Basin (Narkiewicz et al. 2023, Fig. 2H) whereas FAD of *Polygnathus linguiformis* n. ssp. A was established by Walliser and Bultynck (2011, pl. 3. Figure 9) and Narkiewicz et al. (2023, Fig. 2I).

The base of the *hemiansatus* Zone was defined by the first appearance of *Polygnathus hemiansatus* Bultynck, 1987 in sample 14 (Fig. 4l, Sl 1). The presence of this zone is confirmed by *Icriodus obliquimarginatus* (Fig. 5c,d) and *Polygnathus ling. weddigei* (Fig. 5g) found in samples 15 and 16. The representatives of the first taxon appear slightly above the base of the *hemiansatus* Zone (Walliser and Bultynck 2011, p. 17) whereas FAD of the second one falls in the *hemiansatus* Zone (Walliser and Bultynck 2011, pl. 3, Fig. 11). It can be noted that the Eifelian-Givetian boundary has been lowered here relative to the previous concept of Walliser (1990) (Fig. 1).

The base of the *timorensis* Zone is defined by the appearance of *Polygnathus timorensis* Klapper, Philip and Jackson, 1970 in sample 21 (Fig. 5n, Sl 1). Typical representatives of the species indicative of the successive *rhenanus/varcus* Zone have not been found in the studied section. Nevertheless, sample W 22 yielded *Polygnathus linguiformis* aff. *mucronatus* Wittekindt, 1966 (Fig. 5r, Sl 1) which may suggest a proximity of the *rhenanus/varcus* Zone.

The Kačák Episode was first reported from the Pic de Bissous section based on the presence of a distinct cephalopod fauna, including *Cabrieroceras crispiforme*, and species of *Sobolewia* and *Agoniatites* (House and Chlupáč, 1987; House, 1995, 1996). This cephalopod-bearing level (referred to as the *crispiforme* Zone in Fig. 1), is now attributed to the uppermost Eifelian (Walliser et al., 1995). It is here assumed that it corresponds to the onset of the Kačák Episode, in accordance with the concept

proposed by Walliser (1996, 2000). It is coincident with the appearance of the dacryoconarid *Nowakia otomari* and with other bioevents related to the Kačák/*otomari* Event in Bohemia and elsewhere (House and Chlupáč, 1987). Such defined KE lower boundary falls in the *kockelianus* Zone in the studied section (see also Walliser, 1990). Upper part of the KE interval corresponds to the "*ensensis*" Zone whilst its top approximately corresponds to the Eifelian-Givetian boundary defined above. The uncertainty interval comprises the thin Zebra Bed with a poor non-diagnostic conodont assemblage (Fig. 1; SI 1).

# Biodiversity and biofacies of platform conodonts

The evolution of conodont diversity is plotted against the percentage of juvenile forms in particular samples and distribution of biofacies in the section (Fig. 1). The percentage of juveniles in a sample varies around the mean value 49.6%. There are three distinct minima related to the KE interval and followed by a rapid rise to higher values. Near the KE bottom (sample 5A) 34% of juveniles are found, rising to 57% in samples 7 and 7A. Less pronounced change is observed near the base of the "*ensensis*" Zone where the proportion of juvenile forms falls to 29% in sample 8 rising to 41% and 58% in samples 11 and 12, respectively. The top of the KE interval is marked by a distinct rise from 42% in sample 13 to 62% in the closely located sample 14.

The conodont biofacies, particularly the *Icriodus/Polygnathus* ratio, are summarized in the previous paper (Narkiewicz et al. 2023). It may be noted that icriodids are particularly abundant around the base of the KE interval and near the base of the "*ensensis*" Zone (Fig. 1). Above that level they lose importance at the expense of polygnathids, and become more significant only in the uppermost part of the section (sample 23 with 35% of *Icriodus*).

Conodont diversity is here defined as a number of morphological varieties of $P_1$ conodonts described as species, subspecies and/or morphotypes. Included were also taxa determined in an open nomenclature (*affinis*) if they represent distinct varieties which cannot be identified as a certain species, subspecies or morphotype. In exceptional cases the count included also taxa determined on a generic level if the genus was not represented by any species or morphotype in a sample. In such case the number of taxa was arbitrarily set as one. For example in sample 3 *Icriodus* is represented only by 18 specimens determined as *Icriodus* sp. and therefore one *Icriodus* taxon is marked in Fig. 1. This is a rather conservative assumption as the specimens may in fact represent more than one morphological variety of the genus.

Obviously, excluding other elements than $P_1$ imposes limitations on the evaluation of the conodont diversity. Nevertheless, it should be stressed that the taxa other than those defined by $P_1$ elements are rare in the collected material (see Narkiewicz et al., 2023). The only exception is *Belodella* which occurs more abundantly in lower part of the section, contributing to polygnathid-belodellid biofacies.

The diversity pattern (Fig. 1) shows maximum values within and just above the KE interval. Two distinct minima corresponding to the lower and upper boundary of KE are characterized by presence of 4 and 5 taxa, respectively. Such pattern may reflect, at least partly, the dependence between the conodont abundance in the samples and the taxonomic diversity of respective asemblages. The positive

correlation between both parameters seen in Fig. 1 is confirmed by a correlation coefficient exceeding 0.5. This may be explained by the obvious observation that, in general, low conodont frequency per sample may exclude some taxa, particularly those occurring more rarely in the living assemblage sampled. For this reason sample 24 with the frequency of merely14 specimens, has not been considered in further analysis. Moreover, it is to be stressed that lowered conodont frequency in sample 13 may be partly caused by the unique lithology of the Zebra Bed. Considerable proportion of the rock, visually estimated as 60–70%, is a crystalline calcite cement, and thus the conodont yield from the remaining volume of sediment is not quite comparable with other samples of the same weight.

Within the KE interval there is a subordinate diversity minimum (sample 8 with seven taxa) which is not easily explainable by a low conodont frequency. Above this sample the diversity rises to 9 taxa in sample 10 and reaches the maximum of 12 taxa in sample 11. Notably, this abrupt increase over a short vertical distance corresponds to a change from icriodid-dominated to polygnathid-dominated biofacies (Fig. 1). It is also associated with appearance of *Polygnathus ling. klapperi* characteristic for the uppermost Eifelian.

To minimalise the frequency effect on the diversity pattern we adopted the procedure of Suttner et al. (2017) by counting range-through taxa. The latter include also taxa and morphotypes not present in the given sample but encountered in the samples below and above it. Such “ghost” taxa would be expected to occur if a conodont assemblage were more representative, i.e. more abundant in our case. The obtained “potential diversity” curve shows increase from 8 to 13 taxa at the lower KE boundary, with a plateau of 12 forms in the KE interval. The increase is associated with the appearance of new taxa: *Icriodus hollardi*, *I. regularicrescens* and *Polygnathus amphora*. The second rise, to the maximum of 15 taxa just above the Eifelian-Givetian boundary, is marked by the appearance of *Polygnathus hemiansatus*, *P. pseudofoliatus* γ morphotype, *P. ling. weddigei* and *P. obliquimarginatus*. Also, *Ozarkodina bidentata, Tortodus* cf. *T. obliquus* and *P. eiflius* have their single occurrences at this level. In the upper part of the *hemiansatus* Zone the diversity drops to 9 taxa in samples 22 and 23.

# Interpretation and discussion

The reason for the conodont frequency fluctuations connected with the Kačák Episode interval (Fig. 1) is not obvious given a continuous sedimentation and rather uniform facies development throughout the section. The lower frequency minimum, particularly noted in sample 5, may be related to environmental changes accompanying the KE onset, e.g. changing redox conditions in a water column. Sample 12 with an exceptional conodont abundance comes from coarse-grained skeletal calcarenite – packstone-grainstone. It is possible that it represents lag deposit enriched in heavy fraction due to sediment winnowing under regressive conditions of the late KE (Narkiewicz et al., 2021). On the other hand, frequency decrease in the Zebra Bed can be explained by its peculiar lithology (see above) and, consequently, exceptional conditions during deposition. In turn, the higher values noted just above the base of the early Givetian *hemiansatus* Zone (samples 14–16) may be related to lower depositional rates suggested by the concentration of macrofaunal remains including cephalopods. This in turn may have

been caused by the eustatic sealevel rise resulting in more distant terrigeneous sediment sources and less efficient carbonate-sediment factory.

Due to a possible bias caused by underestimated $P_1$ diversity in less abundant assemblages (see above), more attention is paid here to the potential diversity distribution including range-through taxa (Fig. 7). The latter is here regarded as more representative for the diversity changes in the studied section. Distinct increase in such defined diversity is clear at the base and just above the KE interval. Similar two-step pattern is observed in one of three Middle Devonian localities in the Carnic Alps investigated by Suttner et al. (2017), the Zuc di Malaseit Basso (ZMB) comprising the carbonate distal slope sediments. Taking into account depositional and conodont biofacies characteristics ZMB appears most similar to the Pic de Bissous section. The other two localities represent either shallow-marine reefal deposits, particularly in the lower Givetian part (Val di Collina Quarry), or strongly condensed pelagic sediments with a probably reworked fauna (Wolayer “Glacier” section; Suttner et al. 2017). In the first case the conodont assemblage appears impoverished due to shallow-water conditions. In the secon, the pelagic assemblages may include stratigraphically mixed conodonts, and thus unsuitable for reconstructing temporal biodiversity changes.

In the ZMB section the “species abundance” (including the range-through taxa) is mostly between 18 and 20 taxa in the upper Eifelian to lower Givetian interval. It increases by three taxa just below the *ensensis* Zone and by two taxa near the Eifelian-Givetian boundary. The peak diversity of 24 species in the uppermost *ensensis* Zone is followed by a drop to 21 species in the lowermost *hemiansatus* Zone, and thus appears earlier than in the Pic de Bissous section. Thus, although the two-step increase in diversity associated with the KE boundaries seems similar in both compared sections, their exact timing seems to be slightly different.

Lack of a precise correspondence between the present results and those of Suttner et al. (2017) is probably caused by differently defined pool of conodont forms included in the biodiversity analysis. In the present contribution only the $P_1$ taxa and morphotypes were taken into account while in the discussed study coniform and ramiform taxa were considered as well. In addition, the ZMB section embraces larger stratigraphic interval (Eifelian *australis* to middle Givetian *ansatus* zones) and therefore the range-through forms include more long-ranging taxa than in Pic de Bissous section. For the above reasons the overall potential conodont diversity is markedly larger in the case of ZMB data in spite of its similar facies setting and conodont biofacies composition.

On the other hand, the lack of a precise chronostratigraphic correlation of both discussed sections may result from different taxonomic and biostratigraphic concepts (particularly concerning the “*ensensis*” Zone) and resulting correlation errors. Lastly, it can be noted that the cited authors do not report conodont frequency per weight-normalised sample, and therefore it is impossible to evaluate potential bias in diversity changes in the ZMB section due to fluctuating frequency. Nevertheless, the general pattern of a two-step diversity increase in both compared section is rather striking and is regarded as

meaningful here. Such common pattern in two distant sections suggests that it may have supraregional significance, being controlled by some global events related to the KE interval.

The diversity increase near the lower boundary of the Kačák Episode may have been controlled by the eustatic If transgression of Johnson et al. (1985) (e.g. Walliser 1996; Narkiewicz et al. 2021). Notably, it is associated with the introduction of new taxa, FADs of *I. hollardi* and *P. amphora* (Fig. 7), as well as probably *P. eiflius* and *P. ling. linguiformis γ3* (Fig. 6). On the other hand, the diversity rise in the earliest Givetian may be related to the transgressive event post-dating the terminal Eifelian regression (Narkiewicz et al. 2021). The new conodont forms appearing at this level include *Polygnathus hemiansatus*, *P. pseudofoliatus* γ morph., *P. linguiformis weddigei* and *P. obliquimarginatus* (Fig. 7). The subordinate diversity rise (samples 10 and 11) is marked by the entrance of important form *P. ling. klapperi* and change from I-P to P-I biofacies (Fig. 1).

The causal relationship between the transgressions and biodiversity increase due to radiations and evolutionary innovations in a marine fauna is commonly accepted in the literature (see e.g. Smith 2007). Since the Newell's (1952) hypothesis it has been often explained by expansion of habitable area creating more niches available for colonization. In the case of conodont faunas this phenomenon has been confirmed e.g. for Permian and Triassic (Orchard, 2007) and Middle Devonian (Klapper and Johson 1980). The increase of diversity in the lowermost *hemiansatus* Zone may have been fostered by the previous termination of several typical Eifelian species, like *Tortodus kockelianus kockelianus*, *Polygnathus trigonicus, P. angustipennatus* and *P. robusticostatus* (Fig. 6) thus emptying niches for new taxa.

The pattern of juvenile conodont percentage shows two major minima and one subordinate low followed by rapid increases ("events" shown in Fig. 7). The rise in proportion of juvenile forms can be explained by increased mortality rates among immature individuals which may have different biotic and abiotic causes (Hoffman 1976). In the case of conodonts the abiotic events are often considered, namely the onset of adverse environmental conditions (e.g. Merrill and Powell 1980; Karadi et al. 2020). Notably, the earliest and latest "events" are correlated with the boundaries of the KE interval. It is thus tempting to link the earlier rise in a juvenile mortality rate with the introduction of oxygen-poor conditions accompanying sealevel rise at the onset of the KE interval (House, 1996 Walliser 1996). Likewise, a rapid environmental change associated with the sealevel rise may have been also responsible for the earliest Givetian increase of the juvenile-mortality rate (Fig. 7).

In both cases there is coincidence between the start of possible infavourable conditions with the beginning of increased conodont diversification pulses as discussed above. This appears rather contradictory, as increased biodiversity is thought to correlate with favourable conditions rather then adverse environmental events. This apparent contradiction may be reconciled assuming difference in global versus local scale of possible controls. The global changes related to the KE interval, particularly the eustatic transgressions may have promoted the increased conodont biodiversity worldwide. At the same time they could lead to adverse environmental conditions locally, e.g. due to oxygen-defficiency or

some biotic factors like predation or intensified competition. Nevertheless, the question of possible factors influencing observed mortality pattern of conodonts requires further sedimentological, palaeoecological and geochemical studies.

# Conclusions

Abundant and diverse conodonts collected from the Pic de Bissous section allowed the authors to establish presence of the *kockelianus* Zone of the late Eifelian and *hemiansatus* and *timorensis* zones of the lower Givetian. The "*ensensis*" Zone of the uppermost Eifelian is tentatively defined based on the presence of *Polygnathus linguiformis* n. ssp. A and *P. ling. klapperi*. The location of the Eifelian-Givetian boundary is revised being placed within or just above the characteristic Zebra Bed. Stratigraphic ranges of key taxa important for defining the uppermost Eifelian Kačák Episode (KE) are compiled and discussed.

The diversity of platform ($P_1$) conodonts including range-through taxa shows distinct rises near the lower and upper boundary of the KE interval. The two-step pattern is comparable to the previous results from the Zuc di Malaseit Basso section in the Carnic Alps (Suttner et al. 2017). This suggests global nature of the phenomenon, confirmed by appearance of several new taxa and morphotypes at respective levels. Lower diversity rise coincides with the If eustatic transgression, while the upper one correlates with the presumed eustatic rise in the earliest Givetian. Such diversity pattern is explained by creation of new ecological niches due to expansion of habitable marine area.

The two episodes of a diversity rise are accompanied by events of increasing juvenile conodont mortality documented by a higher percentage of immature specimens in the studied assemblages. The events are interpreted as an effect of adverse conditions occuring on a local/regional scale, such as e.g. low-oxygen habitats or increased predation or competition accompanying diversification events.

# Declarations

### Data availability

The conodont specimens studied are stored in the Polish Geological Institute-NRI (Warszawa, Poland).


### Acknowledgments

This study was supported by the Polish National Science Center within the framework of the project no. 2018/29/B/ST10/00411. Partial financial support was provided by the Polish Geological Institute-NRI statutory funds (PGI-NRI Project 61.2908.1802.15). Peter Königshof kindly provided access to the collections stored in the Senckenberg Research Institute and Natural History Museum in Frankfurt. Jiří Kalvoda is acknowledged for making available his conodont collection from the Jirásek Quarry. We thank Krystian Wójcik (PGI-NRI Warszawa) for performing part of the fieldwork and for computer graphics.

# References


1. Bischoff, G., & Ziegler, W. (1957). Die Conodontenchronologie des Mitteldevons und des tiefsten Oberdevons. *Abhandlugen des Hessischen Landesamtes für Bodenforschung 22*(16), 1–135.
2. Brice, D., Bultynck P., Deunff J., Loboziak S., & Streel M. (1979). Données biostratigraphiques nouvelles sur le Givétien et le Frasnien de Ferques (Boulonnais, France). *Annales Societe Géologique Nord 108*, 325–343.
3. Bultynck, P. (1987). Pelagic and neritic conodont successions from the Givetian of pre-Sahara Marocco and the Ardennes. *Bulletin de l' Institut royal Sciences Naturelles de Belgique, Sciences de la Terre 57*, 149–181.
4. Bultynck, P., & Hollard, H. (1980). Distribution comparée de Conodontes et Goniatites dévoniens des plaines du Dra, du Ma'der et du Tafilalt. *Aardkundige Mededelingen 1*, 1–54.
5. Casier J-G., Préat, A. (1996). Ostracodes et sédimentologie au passage Eifélien-Givétien dans la marbrière du Pic de Vissou (Montagne Noire, France). *Bulletin des Centres de recherches exploration-production Elf-Aquitaine*, *Mémoire 20*, 367–387.
6. Clausen, C.-D., Leuteritz, K., & Ziegler, W. (1979). Biostratigraphie und Lithofazies am Südrand der Elsper Mulde (hohes Mittel- und tiefes Oberdevon; Sauerland, Rheinisches Schiefergebirge). *Geologisches Jahrbuch, reihe A 51*, 3–37.
7. Feist, R. (2003). Biostratigraphy of Devonian tropidocoryphid trilobites from the Montagne Noire (southern France*). Bulletin of Geosciences 78*, 431–446.
8. Feist R. (2002). The Palaeozoic of the Montagne Noire, Southern France. *IGCP 421, North Gondwana mid-Palaeozoic Biodynamics and ECOS VIII, 8$^{th}$ European Conodont Symposium. Guidebook of the Field Excursion. Institut des Sciences de l'Evolution, University of Montpellier II, Montpellier, France,* 1-92
9. Feist R., & Klapper, G. (1985). Stratigraphy and conodonts in pelagic sequences across the Middle-Upper Devonian boundary, Montagne Noire, France. *Palaeontographica*, *A 188*, 1–18.
10. Golonka, J., & Gawęda A. (2012). Plate tectonic evolution of the southern margin of Laurussia in the Paleozoic, In: E. Sharkov (Ed.), *Tectonics – Recent advances*. InTech, 261–282.
11. Hoffman, A. (1976). Mortality pattern of some gastropods from the Badenian (Miocene) Korytnica Clays, Poland. *Neues Jahrbuch für Geologie und Paläontologie, Abhandlungen 152*(3), 293–306.
12. House, M. R. (1995). Devonian precessional and other signatures for establishing a Givetian timescale. *Geological Society, London, Special Publications 85*, 37–49.
13. House, M. R. (1996). The Middle Devonian Kačák Event. *Proceedings of the Ussher Society 9*, 079–084.
14. House, M. R. (2002). Strength, timing, setting and cause of mid-Palaeozoic extinctions. *Palaeogeography, Palaeoclimatology, Palaeoecology 181*, 5–25.
15. House, M. R., & Chlupač, I. (1987). Goniatite faunas relevant to the definition of the Eifelian/Givetian boundary. *Document submitted to the Subcommission on Devonian Stratigraphy, Calgary*, 14, 1–14

16. Johnson, J. G., Klapper, G., & Sandberg C. A. (1985). Devonian eustatic fluctuations in Euramerica. *Geological Society of America Bulletin 96*, 567–587.
17. Kabanov, P., & Jiang, C. (2020). Photic-zone euxinia and anoxic events in a Middle-Late Devonian shelfal sea of Panthalassan continental margin, NW Canada: changing paradigm of Devonian ocean and sea level fluctuations. *Global and planetary change*, *188*, 103153.
18. Kalvoda, J. (1992). The youngest conodont fauna of the Barrandian. *Scripta 22*, 61–63.
19. Karádi, V., Virág, A., Kolar-Jurkovšek, T., & Jurkovšek, B. (2020). Stress-Related Evolution in Triassic Conodonts and the Middle Norian Juvenile Mortality. In J. Guex, J.S. Torday, W.B.Miller, Jr. (Eds.), *Morphogenesis, Environmental Stress and Reverse Evolution*, 37–58. Springer Nature.
20. Klapper, G. (1971). Sequence within the conodonts genus *Polygnathus* in the New York lower Middle Devonian. *Geologica et Palaeontologica 5*(1), 59–79.
21. Klapper, G. (1977). Polygnathus linguiformis linguiformis Hinde, 1879. Synonymy [epsilon morphotype]. In W. Ziegler (Ed.) *Catalogue of Conodonts, III. Schweizerbart* (*Nägele und Obermiller*), *Stuttgart*, p. 465.
22. Klapper, G., & Johnson, J. G. (1980). Endemism and dispersal of Devonian conodonts. *Journal of Paleontology 54*, 400–455.
23. Klapper, G., & Lane, H. R. (1985). Upper Devonian (Frasnian) conodonts of the *Polygnathus* biofacies, N.W.T., Canada. *Journal of Paleontology 59*(4), 904–951.
24. Klapper, G., Philip, G. M., & Jackson, J. H. (1970). Revision of the *Polygnathus varcus* group (Conodonta, Middle Devonian). *Neues Jahrbuch für Geologie und Paläontologie Monatshefte 11*, 1650-667.
25. Merrill, G. K., & Powell, R. J. (1980). Paleobiology of juvenile (nepionic?) conodonts from the Drum Limestone (Pennsylvanian, Missourian-Kansas City area) and its bearing on apparatus ontogeny. *Journal of Paleontology 54*(5), 1058–1074.
26. Narkiewicz, M., Narkiewicz, K., Kruchek, S. A., Belka Z., Obukhovskaya, V. Y., & Plax, D. P. (2021). Late Eifelian Kačák Episode in the epeiric Belarusian Basin: Role of terrestrial-marine teleconnections. *Palaeogeography, Palaeoclimatology, Palaeoecology 562*, Article Number 110106. https://doi.org/10.1016/j.palaeo.2020.110106.
27. Narkiewicz, K., Narkiewicz, M., & Wudarska, A. (2023). Significance of conodont data for explaining geosystem perturbations during the Middle Devonian Kačàk Episode. *Marine Micropaleontology 185*, 102307.
28. Newell, N. D. (1952). Periodicity in invertebrate evolution. *Journal of Paleontology 26*, 371–385.
29. Orchard, M. J. (2007). Conodont diversity and evolution through the latest Permian and Early Triassic upheavals. *Palaeogeography, Palaeoclimatology, Palaeoecology 252*(1-2), 93–117.
30. Schöne, B. R. (1997). Der *otomari*-Event und seine Auswirkungen auf die Fazies des Rhenoherzynischen Schelfs (Devon, Rheinisches Schiefergebirge). *Göttinger Arbeiten zur Geologie und Paläontologie 70*, 1–140

31. Smith, A. B. (2007). Marine diversity through the Phanerozoic: problems and prospects. *Journal of the Geological Society 164*(4), 731–745.
32. Suttner, T. J., Kido, E., Corradini, C., Vodrážková, S., Pondrelli, M., & Simonetto, L. (2017). Conodont diversity across the late Eifelian Kačák Episode of the southern Alpine realm (central Carnic Alps, Austria/Italy). *Palaeogeography, Palaeoclimatology, Palaeoecology 479*, 34–47.
33. Tucker, M. (1974). Sedimentology of Palaeozoic pelagic limestones: the Devonian Griotte (Southern France) and Cephalopodenkalk (Germany). *International Association of Sedimentologists Special Publication 1*, 71–92.
34. Vodrážková, S., & Suttner, T. J. (2020). Middle Devonian (Eifelian, *australis*–*ensensis* zones) conodonts from the Jirásek quarry near Koněprusy (Barrandian area, Czech Republic) with special emphasis on the *Polygnathus pseudofoliatus* Group and notes on environmental changes related to the Kačák Episode. *Bulletin of Geosciences 95*(1), 81–125. Doi: 10.3140/bull.geosci.1774
35. Walliser, O.H., (1990). Marble Quarry at Pic de Bissous. Remarks on stratigraphy. Document submitted to the Subcommission on Devonian Stratigraphy (ICS/IUGS), 2 pp.
36. Walliser, O.H., (1996). Global events in the Devonian and Carboniferous. In O. H. Walliser, (Ed.), *Global events and event stratigraphy in the Phanerozoic. Springer, Heidelberg*, *Berlin*, (pp. 225–250).
37. Walliser, O. H., & Bultynck, P. (2011). Extinctions, survival and innovations of conodont species during the Kačák Episode (Eifelian-Givetian) in south-eastern Morocco. *Bulletin Institut royal des Sciences Naturelles de Belgique, Sciences de la Terre 81*, 5-27.
38. Weddige, K. (1977). Die Conodonten der Eifel-Stufe im Typusgebiet und in benachbarten Faziesgebieten. *Senckenbergiana lethaea 58*, 271–419.
39. Wittekindt, H. (1966). Zur Conodonten-Chronologie des Mitteldevons. *Fortschritte in der Geologie von Rheinland und Westfalen 9*(1), 621–646.
40. Ziegler, W., & Klapper, G. (1976). Systematic Paleontology. In W. Ziegler, G. Klapper, J. G. Johnson. Redefinition and subdivision of the *varcus*-Zone (Conodonts, Middle-?Upper Devonian) in Europe and North America. *Geologica and Palaeontologica 10*, 117–140.

# Figures

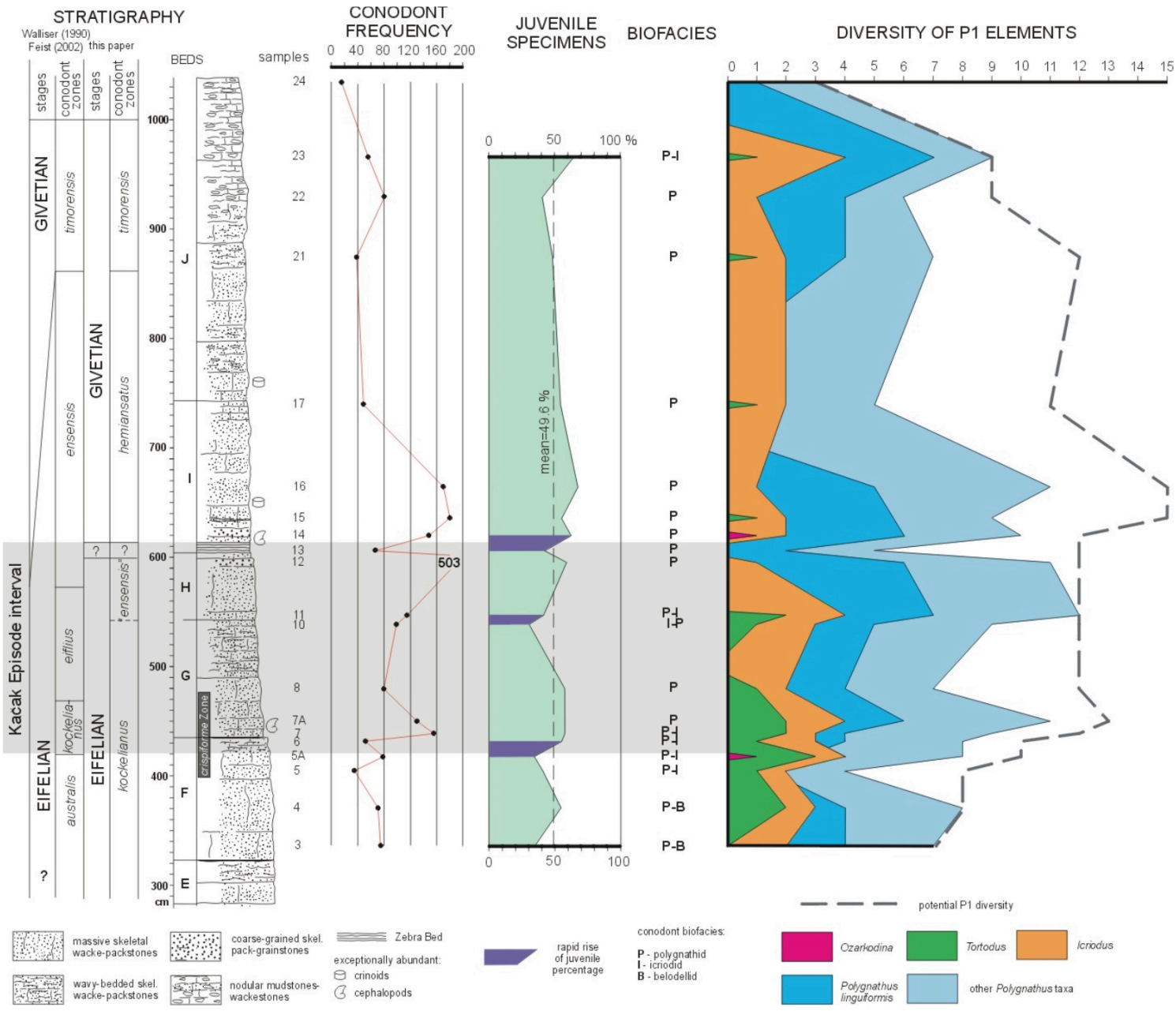


## Figure 1

Stratigraphy of the Pic de Bissous section and conodont data on frequency of P1 elements in samples, percentage of juvenile specimens, biofacies and diversity. Stratigraphy and biofacies partly after Narkiewicz et al. (2023, supplemented and modified). Diversity graph shows number of particular taxa and morphotypes of P1 elements - for further explanation see the text.


## Figure 2

Conodonts from Pic de Bissou, part 1. **a** *Polygnathus linguiformis saharicus* Narkiewicz and Königshof, 2018, sample 3. **b**,**c** *Polygnathus angusticostatus* Wittekindt, 1966, upper and lower views, sample 3. **d**, **e** *Polygnathus angustipennatus* Bischoff and Ziegler, 1957, upper and lower views, sample 3. **f** *Polygnathus linguiformis linguiformis* Hinde, 1879, γ1a morphotype Walliser and Bultynck, 2011, sample 3. **g**, **i**,**n** *Polygnathus pseudofoliatus* Wittekindt, 1966 α morphotype Walliser and Bultynck, 2011, sample

5A; sample 4; sample 10. **h**, **l** *Polygnathus parawebbi* Chatterton, 1974, **h**specimen left-curve, sample 4; **l**specimen right-curve, sample 3. **j**, **k** *Coelocerodonta* sp., sample 4. **m** *Polygnathus pseudofoliatus* Wittekindt, 1966 β morphotype Walliser and Bultynck, 2011, sample 8. **o**, **p**, **q**,**x**, **y**, **z** *Tortodus intermedius* (Bultynck, 1966), **o**, **p**, **q** upper, lower and lateral views, sample 3; **x**, **y**,**z**, upper, lower and lateral views, sample 7. **r**, **s**, **t** *Tortodus kockelianus kockelianus* (Bischoff and Ziegler, 1957), upper view, sample 4; s, t upper and lower views, sample 3. **u** *Ozarkodina brevis* (Bischoff and Ziegler, 1957), sample 5A. **v** *Belodella* sp., sample 3. **w** *Neopanderodus* sp., obverse view, sample 5A. **aa**, **bb**, **cc** *Icriodus hollardi* Walliser and Bultynck, 2011, upper, lower and lateral views, sample 5A. **dd** *Polygnathus linguiformis linguiformis* Hinde, 1879, 3 morphotype Walliser and Bultynck, 2011, sample 6. Scale bar – 100 μm.

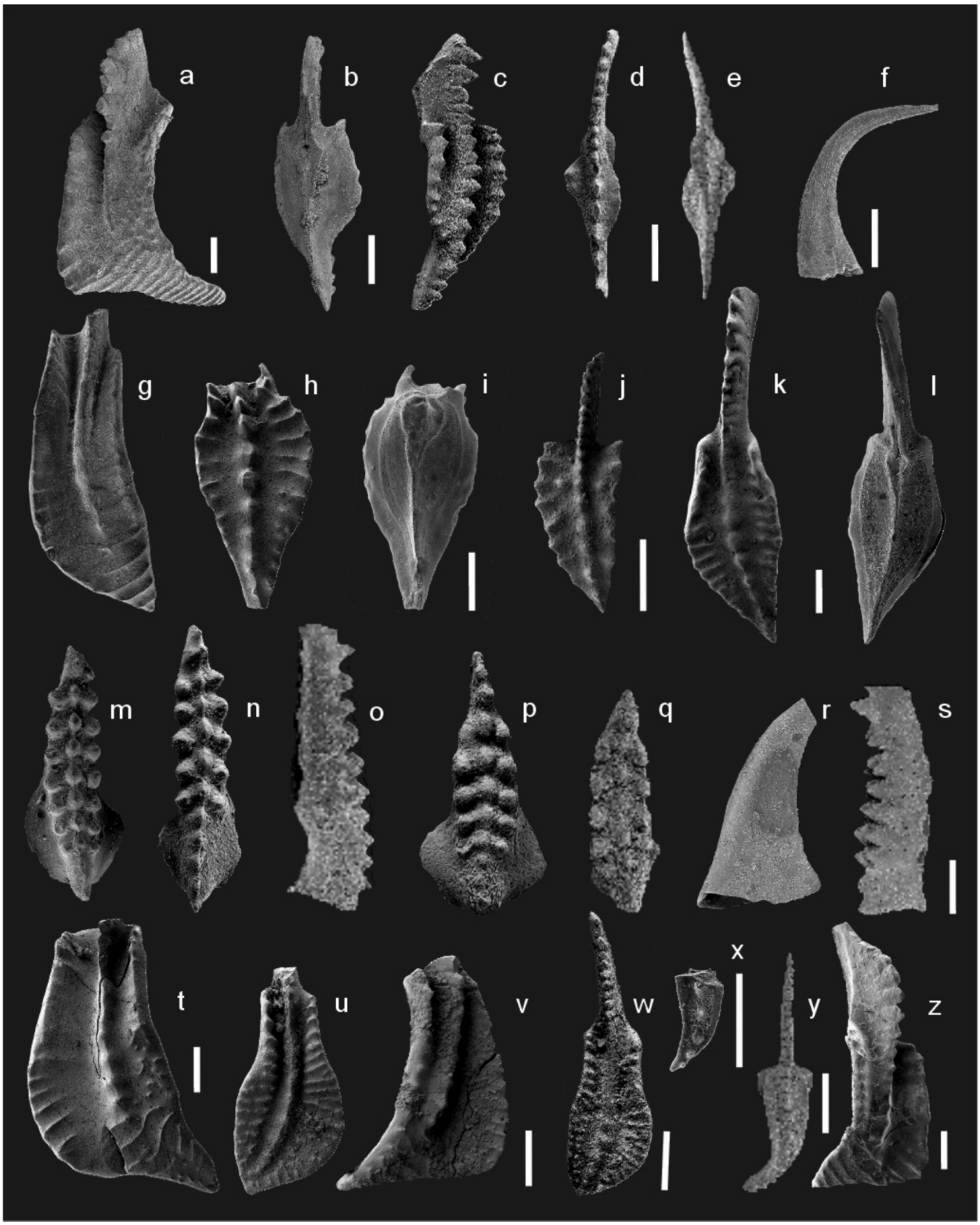


## Figure 3

Conodonts from Pic de Bissou, part 2. **a** *Polygnathus linguiformis* n. ssp. sensu Clausen et al., 1979, pl. 1, fig. 5, sample 7A. **b**, **c**,**d**, **e** *Polygnathus angustipennatus* Bischoff and Ziegler, 1957, **b**, **c**lower and oblique views; **d**, **e** upper and lower views, sample 7A. **f** *Neopanderodus*sp., obverse view of "tortiform" element, sample 7. **g** *Polygnathus linguiformis linguiformis* Hinde, 1879, γ3 morphotype Walliser and Bultynck, 2011, sample 8. **h**, **i**, **k**,**l** *Polygnathus robusticostatus* Bischoff and Ziegler, 1957, **h**, **i**upper and

lower views, sample 7; **k**, **l**upper and lower views, sample 10. **j** *Polygnathus trigonicus* Bischoff and Ziegler, 1957, sample 7. **m**, **n**,**o** *Icriodus regularicrescens* Bultynck, 1970, **m** upper view, sample 10; **n**, **o** upper and lateral views, sample 7A. **p**, **q**, **s** *Icriodus hollardi* Walliser and Bultynck, 2011, **p** sample 7; **q** sample 11; **s** - lateral view of specimen illustrated in Narkiewicz et al., 2023, fig. 2A, sample 10. **r** *Dvorakia* sp., sample 10. **t**, **v** *Polygnathus linguiformis klapperi* Clausen, Leuteritz and Ziegler, 1979, **t** sample 11; **v** sample 12. **u**,**w** *Polygnathus amphora* Walliser and Bultynck, 2011, **u** sample 11; **w** sample 7A. **x**, **y** *Tortodus kockelianus kockelianus* **x** lower part of juvenile specimen, sample 1; **y** sample 8. **z** *Polygnathus linguiformis linguiformis* n. subsp. A sensu Uyeno and Bultynck, 1993, sample 12. Scale bar – 100 µm.

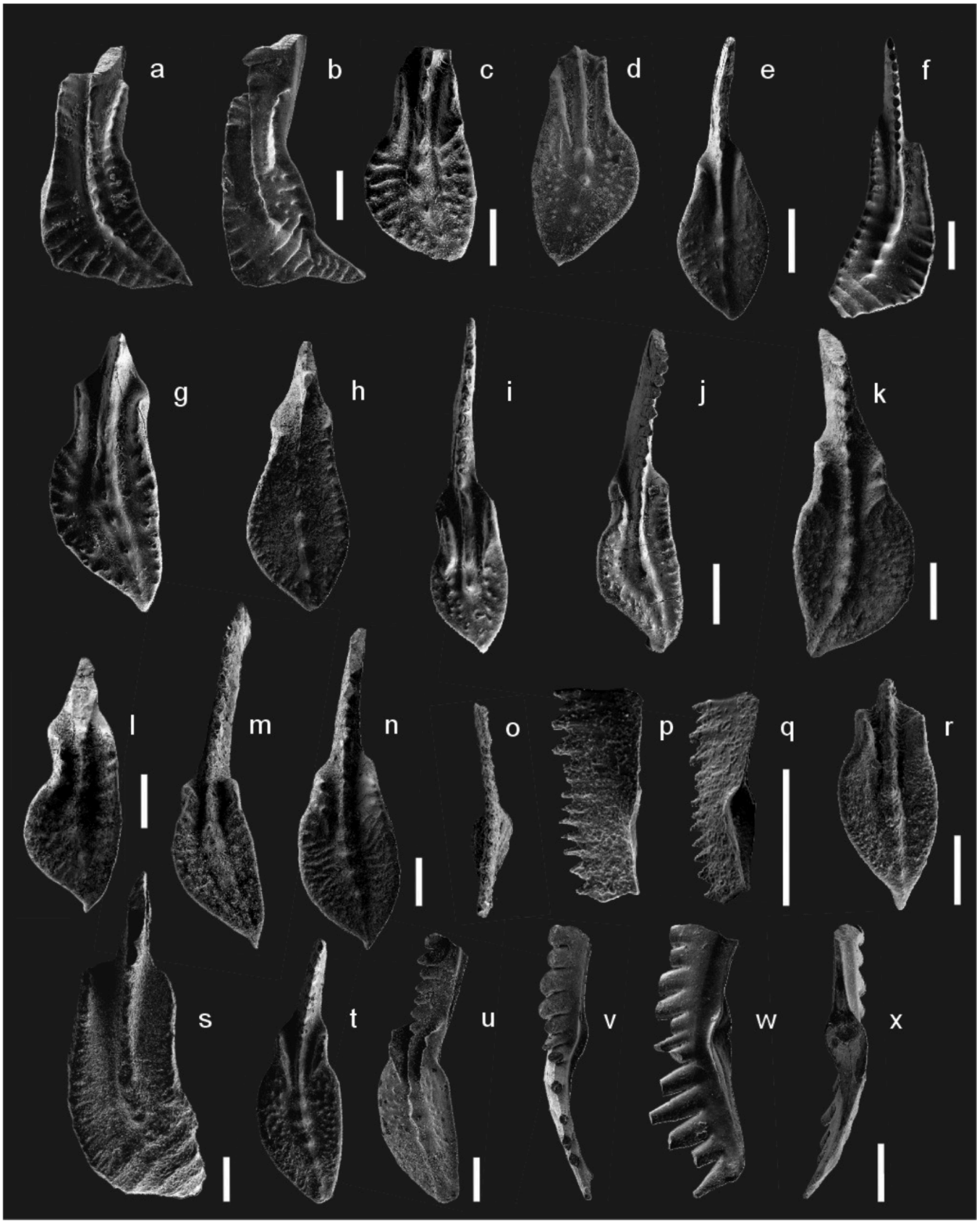


## Figure 4

Conodonts from Pic de Bissou, part 3. **a** *Polygnathus parawebbi* Chatterton, 1974, sample 12. **b** *Polygnathus linguiformis linguiformis* Hinde 1879, γ1b morphotype Walliser and Bultynck, 2011, sample 12. **c**, **d** *Polygnathus pseudoeiflius* Walliser and Bultynck, 2011, **c** sample 13; **d** sample 12. **e** *Polygnathus* sp., sample 12. **f** *Polygnathus linguiformis saharicus* Narkiewicz and Königshof, 2018, sample 13. **g**, **k, n** *Polygnathus pseudofoliatus* Wittekindt, 1966 α morphotype Walliser and Bultynck, 2011, **g** sample 12; **k**,

**n** sample 14. **h**, **i** *Polygnathus amphora* Walliser and Bultynck, 2011, **h** sample 12; **i** sample 13. **j** *Polygnathus* aff. *P. hemiansatus*, the specimen differs from the typical representatives of the species in the lack of a pronounced convex expansion behind outer geniculation point,  sample 12. **l** *Polygnathus hemiansatus* Bultynck, 1987, sample 14. **m**, **r** *Polygnathus pseudofoliatus* Wittekindt, 1966 γ morphotype, sample 14. **o**, **p**, **q** *Ozarkodina bidentata* (Bischoff and Ziegler, 1957), upper, lateral and lower views, sample 14; **s** *Polygnathus linguiformis linguiformis* Hinde, 1879 γ3 morphotype Walliser and Bultynck, 2011, sample 14. **t**, **u** *Polygnathus eiflius* Bischoff and Ziegler, 1957, -upper and oblique views, sample 15. **v**, **w**, **z** *Tortodus obliquus* (Wittekindt, 1966), upper, lateral and lower views, sample 15. Scale bar – 100 μm.

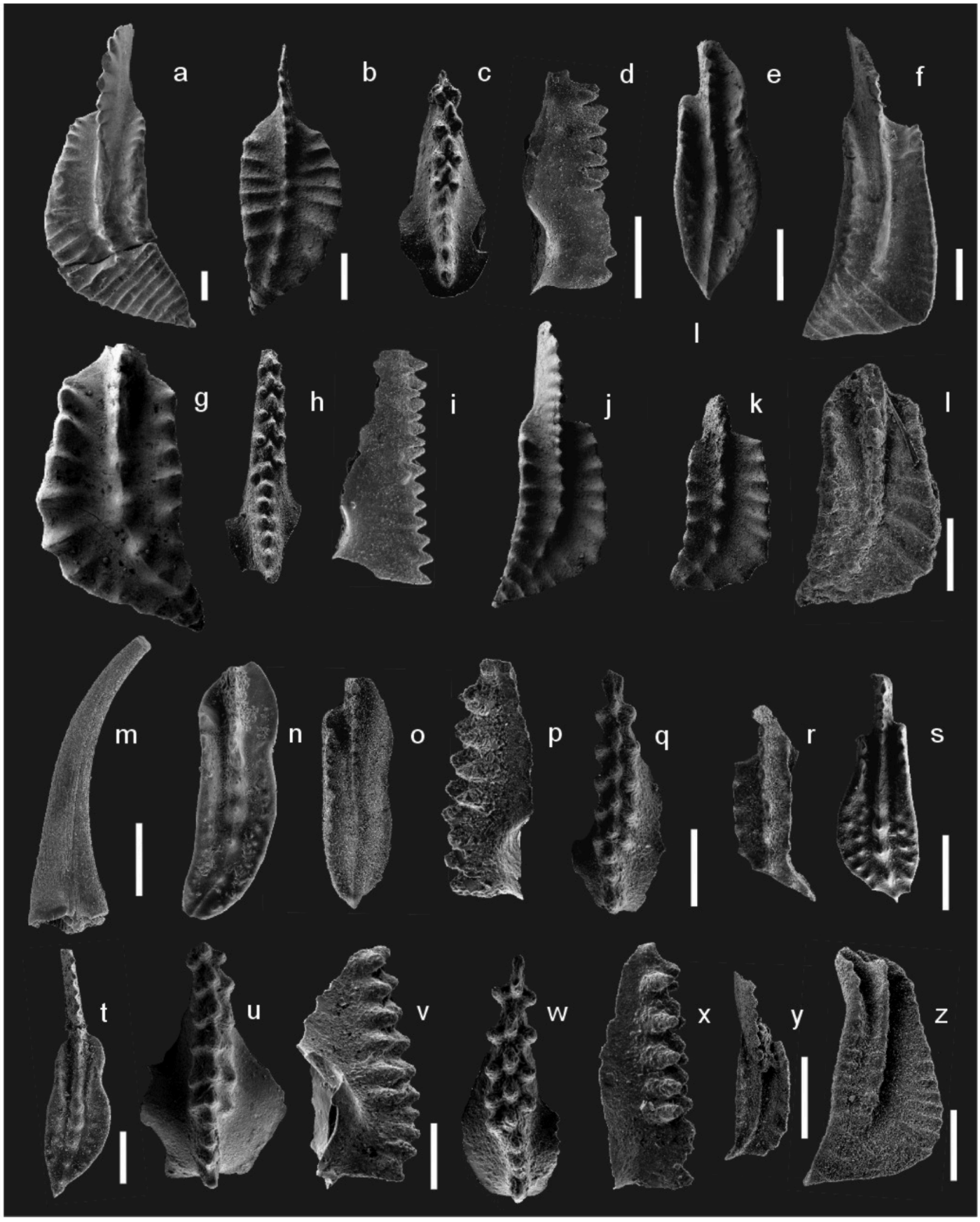


## Figure 5

Conodonts from Pic de Bissou, part 4. **a** *Polygnathus linguiformis klapperi* Clausen, Leuteritz and Ziegler, 1979, sample 21. **b** *Polygnathus kluepfeli* Wittekindt, 1966, sample 16. **c**, **d** *Icriodus obliquimarginatus* Bischoff and Ziegler, 1957 morphotype γ Walliser and Bultynck, 2011, upper and lateral views, sample 15. **e** *Polygnathus hemiansatus* Bultynck, 1987, sample 16. **f** *Polygnathus linguiformis linguiformis* Hinde, 1879 γ1a morphotype Walliser and Bultynck, 2011, sample 22; sample 16. **g** *Polygnathus linguiformis*

*wediggei* Clausen, Leuteritz and Ziegler, 1979, sample 15. **h**, **i** *Icriodus obliquimarginatus* Bischoff and Ziegler, 1957 morphotype β Walliser and Bultynck, 2011 upper and lateral, sample 16; **j**, **k** **l** *Polygnathus linguiformis linguiformis* n. subsp. A sensu Uyeno and Bultynck, 1993, **j**, **k** sample 16; **l** sample 21. **m** *Neopanderodus* sp., obverse view, sample 23. **n**, **o** *Polygnathus timorensis* Klapper, Philip and Jackson, 1970, **n** sample 21; **o** sample 23. **p**, **q** *Icriodus regularicrescens* Bultynck, 1970, lateral and upper views, sample 23. **r** *Polygnathus linguiformis* aff. *mucronatus*, the specimen differs from the typical representatives of *P. linguiformis mucronatus* Wittekindt, 1966 in platform margins being flat and not raised high (see Wittekind, 1966, p. 636, pl. 2, fig. 15 – holotype; Klapper, 1977). **s** *Polygnathus pseudofoliatus* Wittekindt, 1966 γ morphotype, sample 17. **t** *Polygnathus hemiansatus* Bultynck, 1987, sample 24. **u**, **v** *Icriodus regularicrescens* Bultynck, 1970→*Icriodus brevis* Stauffer, 1940, upper and lateral views, sample 23. **w**, **x** *Icriodus eslaensis* Van Adrichem Boogaret, 1967, upper and lateral views, sample 23. **y** *Polygnathus parawebbi* Chatterton, 1974, sample 24. **z** *Polygnathus linguiformis saharicus* Narkiewicz and Königshof, 2018, sample 23. Scale bar – 100 μm.

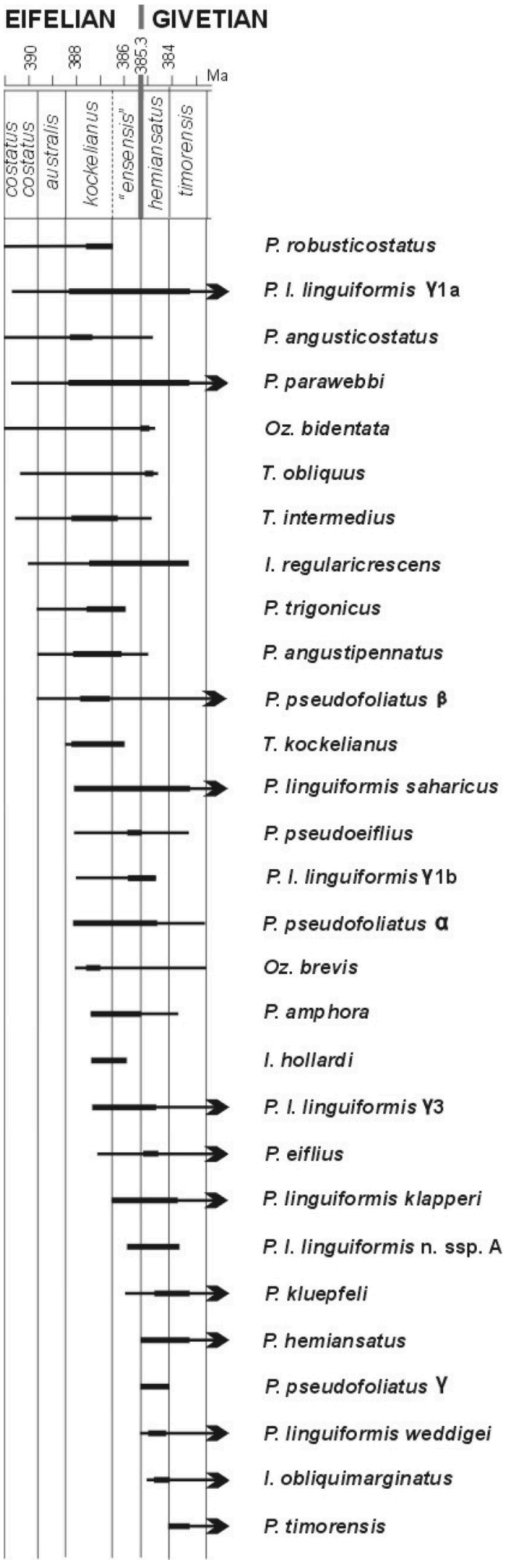


## Figure 6

Stratigraphic ranges of conodont taxa and morphotypes found in the Pic de Bissous section. Observed ranges (bold lines) are shown against total ranges (partly based on Narkiewicz et al., 2023, modified).

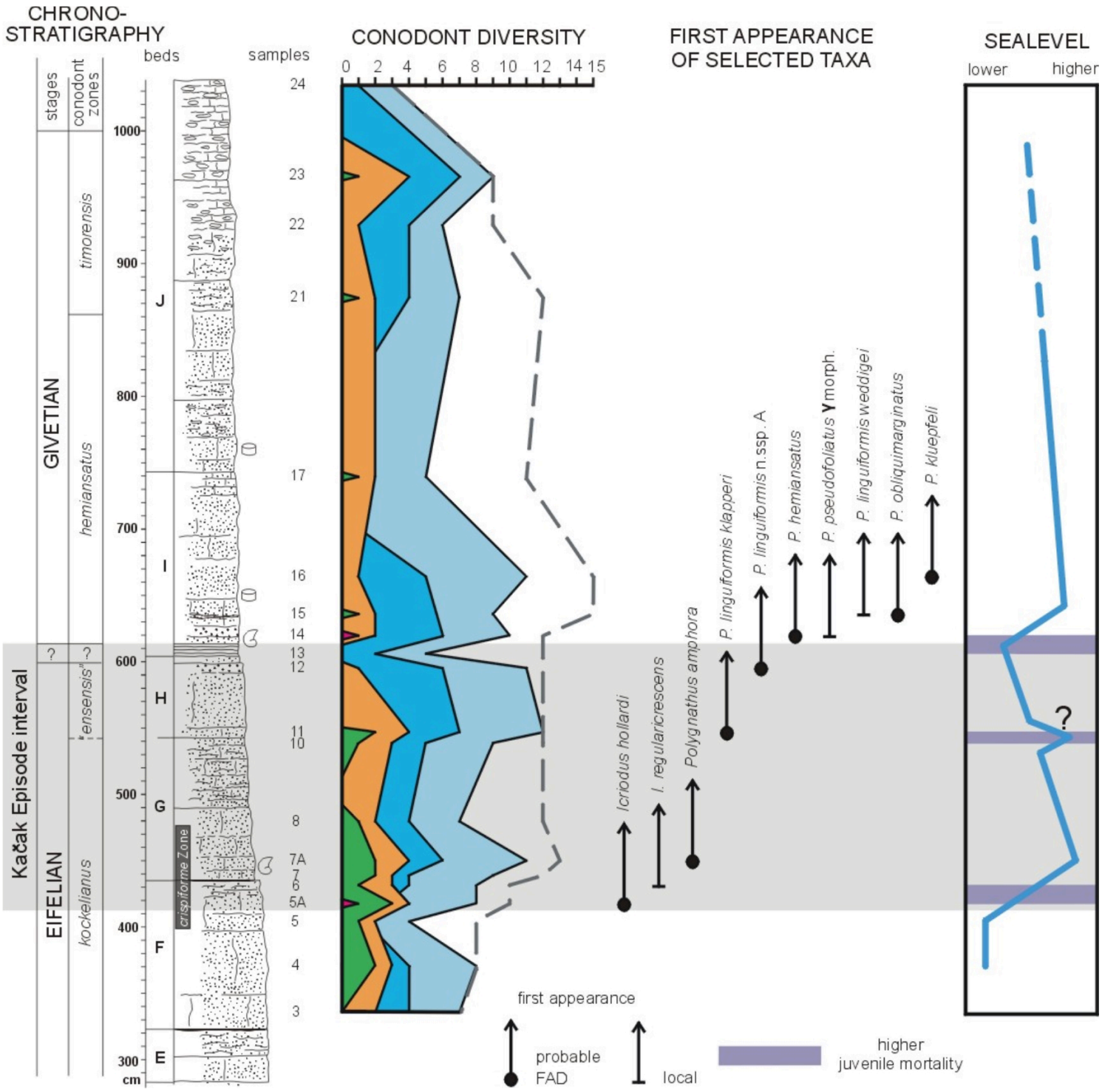


**Figure 7**

Interpretation of conodont data from the Pic de Bissous section in terms of eustatic fluctuations related to the Kačak Episode. For other explanations see Fig. 1.

# Supplementary Files

This is a list of supplementary files associated with this preprint. Click to download.

- NarkiewiczNarkiewiczSM1.pdf